Real time identification of active regions in muscles from high density surface electromyogram

Computers in Biology and Medicine

Real Time Identification of Active Regions in Muscles from High Density Surface Electromyogram

Luca Mesin

Mathematical Biology and Physiology, Dipartimento di Elettronica e Telecomunicazioni, Politecnico di Torino, Corso Duca degli Abruzzi 24, Turin, 10129, Italy.

Running title: Real time localization of EMG sources

Corresponding author:

Luca Mesin, PhD

Department of Electronics and Telecommunications, Politecnico di Torino, Corso Duca degli Abruzzi 24, Torino, 10129 ITALY

Tel. 0039-0110904085 Fax. 0039-0110904099 e-mail : luca.mesin@polito.it

Abstract

Purpose: Developing a real time method for the localization of muscle activity regions from high density surface electromyogram (EMG).

Method: The inverse problem of source localization is solved by a regularized technique applied to an over-determined problem searching for the least mean squares approximation of the recorded signal with a linear combination of a set of basis waveforms (subject specific).

Results: The method, tested on simulations, provides accurate estimates of the mean location of the sources (in ideal conditions, it has about 1 mm of mean error in locating the depth, negligible error in locating the transverse location of the active region). For reasonably small perturbations, it is stable to possible detection problems (e.g., misalignment between the electrodes and the fibres, noise), inaccurate knowledge of the anatomical and physical properties of the investigated tissues (e.g., tissue thickness, location of IZ, fibre length, tissue conductivity) with mean estimation errors of about 1.5-2.8 mm.

Conclusions: An innovative algorithm is proposed for the non-invasive localization of the active regions of a muscle. It is real time and opens potential future applications for prosthesis control and biofeedback.

Keywords: electromyography, inverse problem, source localization, real time

1. Introduction

Surface electromyogram (EMG) is the potential recorded over the skin resulting from the generation (at the innervation zone - IZ), propagation (along muscle fibres, across the membrane), extinction (at the tendon endings) of current sources that induce fibre contraction. High density surface EMG (HDsEMG) has been proposed to investigate the muscle activity on a wide spatial area with a good selectivity [1]. Indeed, spatial filters allow to overcome in part the smaller selectivity with respect to needle EMG [2]. As a results, HDsEMG may find many clinical applications, some of them similar to those of the routinely used needle EMG (e.g., concerning the recruitment strategy of different motor units - MU [3]), but without requiring invasive procedures [4-6]. Moreover, as a wide area is considered, many important features (not attainable from needle EMG) can be extracted, e.g. concerning the anatomy of the muscle (positions of IZ and tendon endings [7-11]) and the velocity of propagation of MU action potentials (MUAP) [12].

An important information on muscle contraction is the position of the active regions. In principle, this information could be extracted from HDsEMG by estimating the location of the current sources generating the surface potential. However, identifying the sources from the recorded EMG is not simple, as it is an inverse problem. The localization of sources within the brain was studied extensively from surface electroencephalogram (EEG) [13]. In the field of EMG, some studies have been proposed [14-20]. The identification of the source of a single MUAP was addressed by considering that the decay of the potential in the transverse direction with respect to the fibres is slower when the MU is deeper [17]. This method requires the (computationally intensive) decomposition of the surface EMG as a preliminary step, if interference EMG is considered. Sophisticated methods, based on advanced simulations by the finite elements method (FEM), were also proposed to investigate interference EMG [14-18]. More recently, FEM simulations combined with regularization techniques were applied [19-20]. All these methods have a high computational cost. Thus, they are not feasible for real time applications, like prosthesis control or rehabilitation

guidance with a biofeedback (where an estimation of the active regions would be beneficial, to improve prosthesis control without introducing an unpleasant delay or to examine the activity of the muscle during a rehabilitation program [20]). As an alternative, a simple and fast method was proposed to estimate the relative depth of the sources from interference surface EMG [21]. Such a method, together with a simple algorithm to estimate the location of the sources in the directions parallel to the skin (e.g., based on the mean amplitude of the signal) could provide real time estimates. However, this approach has some limitations: it provides only relative depth information (i.e., the region activated in a period is deeper or more superficial than in another moment), it gives an average estimate of depth (for example, if there are two active regions at different depths, the information obtained by the method is related to the average depth among the two regions, weighted by the amplitude of the sources and the distance from the detection channels) and it does not estimate the contributions of different sources (that could be useful, e.g. to reduce cross-talk [20]).

Here, an innovative method is proposed to provide a rough localization of the sources of interference surface EMG in real time. It is based on a set of pre-determined waveforms, each associated with a source in a specific location (as in [14][18]), recorded by a HDsEMG system (with number of electrodes higher than the number of waveforms). A regularization method is used, in order to stabilize the estimates (as in [19][20], where an expensive FEM model is used). The problem is stated in terms of the minimization of a functional in the least mean squares sense, whose solution is achieved with a series of matrix multiplications, which can be obtained quickly, opening new potential real time applications.

2. Materials and Methods

The method and the simulated signals used to test it are described in the following.

2.1 Algorithm for source localization

Assume to describe the recorded EMG $b(x,t)$ by the following expression

$$b(x,t) = \sum_{n=1}^{N_R} \sum_{k=1}^{N_\tau} X_{n,k} a_n(x, t - \tau_{nk}) \quad (1)$$

where $a_n(x,t)$ is a normalized waveform representing the activity of fibres in a specific muscle region (N_R is the number of regions considered), x is the space variable indicating the position of the recording channel, t is the time variable, τ_{nk} is a delay (N_τ is the number of considered delays), $X_{n,k}$ are unknown coefficients to be determined, indicating which muscle region is active and the average intensity of the source. The functions $a_n(x,t)$ (referred to as basis waveforms in the following) could be simulated using a model replicating as far as possible the investigated physiological system: for example, the geometry of the tissues could be measured (by ultrasound scanning [22] or MRI [15][16][18-20][23]), their conductivity could be taken from the literature [24][25] and the anatomy of the muscle fibres (positions of the IZ and tendons) could be investigated by preliminary surface EMG recordings [8-11]. Another possible choice is to measure the surface potential resulting from the activity of a specific region: needle EMG can be recorded from different locations and decomposed in order to identify the activity of single MUs [26]; then the surface response related to each identified MU can be estimated by spike triggered averaging [27], obtaining very selective information on the surface EMG response of the activity of specific muscle regions.

Equation (1) can be rewritten in matrix form

$$AX = b \quad (2)$$

where A contains the basis waveforms, b the measurements, X the unknowns

$$A=\begin{bmatrix} \uparrow & & \uparrow & \uparrow & & \uparrow & & \uparrow \\ a_1(x,t-\tau_1) & \cdots & a_1(x,t-\tau_{N_\tau}) & a_2(x,t-\tau_1) & \cdots & a_2(x,t-\tau_{N_\tau}) & \cdots & a_{N_R}(x,t-\tau_{N_\tau}) \\ \downarrow & & \downarrow & \downarrow & & \downarrow & & \downarrow \end{bmatrix}$$

$$X=\begin{bmatrix} X_{1,1} \\ \vdots \\ X_{1,N_\tau} \\ X_{2,1} \\ \vdots \\ X_{2,N_\tau} \\ \vdots \\ X_{N_R,N_\tau} \end{bmatrix} \qquad b=\begin{bmatrix} \uparrow \\ b(x,t) \\ \downarrow \end{bmatrix} \tag{3}$$

where the arrows indicate that a vector is formed listing the values corresponding to each detection channel and time sample.

There are some problems in solving the linear system (2): inverting A is not possible because it is usually rectangular; the measurement vector b is not in the image of A, as it should be smooth (as it is the solution of a problem of potential [28]), but it is not, due to the noise (always present in the experimental data [29]).

The problem could be solved in the least mean squares sense

$$\min_X \quad \|AX-b\|^2 \tag{4}$$

with solution

$$X=\left(A^TA\right)^{-1}A^Tb \tag{5}$$

However, this solution could result in many contributions, which compensate each other. In order to get a reliable solution, a-priori information can be included by introducing penalization terms and imposing constraints [13]. Tikonov regularization is obtained solving the following problem

$$\min_X \underbrace{\|AX-b\|^2}_{\substack{\text{residual}\\ \text{norm}}} + \alpha \underbrace{\|X\|^2}_{\substack{\text{solution}\\ \text{norm}}} \tag{6}$$

in which the solution is imposed not to have a large norm (ruling out oscillating solutions), by properly tuning the penalization parameter α (equal to the maximum eigenvalue of the matrix A^TA divided by 1000, in this paper). The problem has an analytical solution obtained considering that

$$\|AX-b\|^2+\alpha\|X\|^2=\left\|\begin{bmatrix}A\\ \sqrt{\alpha}I\end{bmatrix}X-\begin{bmatrix}b\\ 0\end{bmatrix}\right\|^2=\|BX-c\|^2 \tag{7}$$

from which we have

$$B^TBX=B^Tc \quad \Rightarrow \quad \left(A^TA+\alpha I\right)X=A^Tb \quad \Rightarrow \quad X=\left(A^TA+\alpha I\right)^{-1}A^Tb \tag{8}$$

This solution is less sensitive to noise than (5) (as the condition number of the matrix to be inverted was decreased), but it could have unphysical negative values. To avoid this problem, the solution was constrained to be non-negative. The projected Landweber method [30] was used. It updates the solution in the direction of steepest descent of the square error functional and then employs projections onto the constraint set, i.e. the non-negative orthant, which is a closed convex set. The algorithm is the following

$$\begin{cases} Initializa\,tion: X_0 \\ y_{k+1}=X_k-\mu A^T(AX_k-b), \quad \mu=\dfrac{0.9}{\lambda_{\max}(A^TA)} \\ X_{k+1}=\max(y_{k+1},0) \end{cases} \tag{9}$$

where the initialization for X_0 is given by the Tikonov method (Equation (8)), $\lambda_{\max}(A^TA)$ is the maximum eigenvalue of the square matrix A^TA, the step size parameter μ was chosen in order to achieve convergence in a few steps (5 iterations were used here) and the maximum operator in the definition of X_{k+1} is evaluated component-wise [30]. In order to have a fast algorithm, the matrix A is obtained considering a fixed geometry and a constant velocity of propagation of the current sources along the fibres (4 m/s). Thus, the matrix $M=\left(A^TA+\alpha I\right)^{-1}A^T$ (needed to compute the Tikonov solution (8)), the matrix A^TA and its maximum eigenvalue can be computed before the application of the method to the signals. As a result, the algorithm (9) consists only of a few matrix multiplications, which could be performed very quickly (see the Results section for details).

As the considered geometry is fixed, the method could be applied in isometric conditions or in situations in which the movement is limited. If dynamic conditions are considered, a set of matrixes could be saved, each corresponding to a specific geometrical configuration of the muscle fibres and

the matrix corresponding to the actual condition could be selected on the basis of the measured joint angle. In the following, isometric conditions are simulated (however, the effect of different IZ positions and fibre lengths is considered).

The average muscle fibre conduction velocity (CV) can change during a contraction, for example due to the recruitment of different MUs with different CV (e.g., when a non-isotonic contraction is studied [31]) or as a myoelectric manifestation of muscle fatigue [32]. Muscle fibre CV was estimated from the linear electrode array aligned to the muscle fibres that corresponded to the maximum average rectified value (ARV). CV was computed with a multichannel least mean squares approach [33], applied to monopolar signals to which the common mode (CM) was subtracted. This method, tested on a few signals, appeared to be more stable than applying the algorithm to double differential (DD) signals (as often done in the literature [33]). This is probably due to the larger number of monopolar channels and to a lower effect of noise with respect to DD (fully testing this hypothesis is beyond the aims of this paper). For the specific application considered here, using monopolar signals is beneficial also because they have a larger detection volume than DD. Once an estimate of CV was obtained, all the signals were rescaled in time in order to compensate the CV variation with respect to the simulated waveforms. In different tests, CV compensation was included or excluded, indicating the effect of such an additional step.

Another important consideration is required on the number of conditions and of unknowns in the inverse problem to be solved. Preliminary tests indicated that more accurate results were obtained using an over-determined system. The number of measurements (equal to the number of rows in the matrix *A* and reflecting conditions) is given by the number of detection channels (most of the tests, described in Section 2.2.1, were performed considering 9 linear arrays of 7 monopolar channels, aligned to the fibres) multiplied by the number of time samples in the considered epoch of signal (indicated by τ_{EPOCH} in the following). The number of unknowns (equal to the number of columns in the matrix *A*) is given by the number of waveforms considered (given by the number of considered depths multiplied by the number of positions along the direction transverse to the fibres), multiplied

by the number of time delays. In most of the simulation tests (Section 2.2.1), I considered 6 depths (one every 2 mm, in the range 1 to 11 mm), 9 transverse displacements (one every 8 mm, from -32 to 32 mm), delays from $-\tau_{WF}$ to τ_{EPOCH}, where τ_{WF} is the duration of a simulated waveform (defined as the simulated length of the fibre divided by CV plus 10 ms, added in order to consider the time needed for the generation/extinction of the source). This range of delays includes all non-zero contributions of the waveforms to the recorded potential. In order to decrease the number of unknowns, the delays were down-sampled of a factor 2 with respect to the sampling rate. In this way, considering a number of source positions to be estimated less than or equal to the number of channels in the detection grid, the linear system (2) is over-determined, irrespective to the duration of the epoch.

As an estimate of the dimensionality of the problem, consider the case of processing an epoch of signal with duration 100 ms: the number of conditions is 9 (arrays) x 7 (channels) x 100 (number of samples in the epoch, sampled at 1 kHz) = 6300; the number of unknowns is 6 (depths) x 9 (transverse displacements) x 60 (number of considered delays, equal to 50, which is the number of samples in an epoch sampled at 500 Hz, plus 10 samples to cover a waveform) = 3240.

2.2 Simulated signals

To test the algorithm, interference surface EMG was simulated. A plane layer volume conductor model was used to simulate single fibre action potentials (SFAP) [34], assuming time sampling frequency of 1 kHz and muscle fibre CV equal to 4 m/s. The conductivity of the tissues were the followings: skin thickness 1 mm, conductivity $2.2 \cdot 10^{-2}$S/m [24]; fat thickness 3 mm, conductivity $4 \cdot 10^{-2}$S/m [24]; muscle longitudinal conductivity $40 \cdot 10^{-2}$S/m and transverse conductivity $9 \cdot 10^{-2}$S/m [25].

A sensitivity analysis (Section 2.2.1 below) was performed on the basis of a dataset simulating an active region moving around the muscle. The geometry of the volume conductor is shown in Figure 1A. The performances of the algorithm in localizing the centroid of the active region were tested

(Figures 2-7). Then, a specific example of application was considered (Section 2.2.2), in which 4 distinct muscles were considered and all their possible co-activations were simulated (Figure 8). The algorithm was used to identify which muscle was active in order to discriminate between different activation patterns (Table 1).

2.2.1 Sensitivity analysis

Monopolar surface EMGs were simulated as detected by a two dimensional grid of 9 parallel arrays of 7 electrodes, centred at 25 mm distal to the IZ, aligned to the muscle fibres, with 8 mm inter-electrode distance (IED, Figure 1A). Muscle fibres were simulated inside a rectangular cross-section area with 70 mm of lateral extension and 10 mm of maximal depth. Symmetrical muscle fibres (with IZ half way between the tendons) were simulated with semi-length 50 mm.

Each SFAP was used to simulate single MUAPs, approximating the smoothing due to the spread of the IZs and tendon endings (8 mm) by a time convolution with a Gaussian window function [32]. The number of fibres in the MUs was distributed as an exponential function [35], with the largest MU including a number of fibres 20 times greater than that of the smallest one. The distribution of single MU CV was assumed to be Gaussian, with a mean of 4 m/s and standard deviation of 0.3 m/s. MUs were recruited according to the recruitment threshold excitation function proposed in [35] with range of thresholds equal to 60%. The discharge statistics were modelled assuming minimum and maximum discharge rates of 8 and 35 pulses per second (pps), a linear increase of the discharge rate with force once the MU was recruited (0.5 pps/% of maximal voluntary contraction - MVC, between the minimum and maximum rates stated above) and a Gaussian distribution of the inter-pulse interval variability (coefficient of variation equal to 0.2). The MUs were recruited from low to high CV [36].

An interference surface EMG of duration 20 s was simulated, imposing a contraction level of 50% of MVC (a few tests with different contraction levels provided equivalent results). Different regions within the muscle were activated during the simulation. Specifically, the simulation time was

divided into 100 epochs. In each epoch, only the MUs included in a specific region were activated: such a region was an ellipse with semi-axes 2.5 and 10 mm, in the depth and transverse direction respectively, as shown in Figure 1B. The active region was displaced during the simulation so that its centre toured around an elliptical path, with semi-axes 4 and 30 mm, in the depth and transverse direction, respectively (Figure 1B).

The algorithm was applied to non-overlapped epochs of the simulated surface EMG of 50, 100 or 150 ms, in different tests. In order to check the accuracy of the algorithm in detecting the active region, for each epoch, the mean position of the firing MUs was computed and compared to the mean of the estimated distribution (cumulated over the considered time delays and removing the values under the 30% of the maximum, in order to reduce the contribution of noisy estimates and of the blurring). The mean and the standard deviation of the distances (across different epochs) between the mean position of the firing MUs and the mean of the estimated distribution was considered to measure the performance of the method.

First, a reference test was considered in which the basis waveforms were obtained using the same simulation model as that used to simulate the MUAPs. Then, a sensitivity analysis was performed, assuming that there was a mistake between the actual investigated physiological system and the simulated or experimental waveforms used to fit the EMG data (by Equation (1)). Indeed, errors could be done in estimating the geometry or the conductivity of the tissues and the anatomy of the investigated muscle fibres. The same simulated interference signal was considered for the tests, but different models were used to simulate the waveforms included in the matrix A in (3). The following parameters were changed one at a time or altogether, in different sets of simulations: skin thickness, fat thickness, skin conductivity, muscle conductivity, IZ location and fibre length. Moreover, technical problems were considered: misalignment of the detection system with respect to the fibres and Gaussian additive noise was added to the interference EMG (with SNR between 10 and 25 dB). In order to test the effect of a change on CV, instead of using the reference CV of 4 m/s

(which is equal to the average CV of the simulated MUs), a different CV (between 3 and 5 m/s) was used to simulate the waveforms.

Moreover, different spatial filters were considered, as an alternative to the monopolar potential used as a reference (which assumes a common reference electrode for all channels): a variation of the monopolar derivation (borrowed from EEG), using the average potential across all electrodes as the reference (it is the so-called virtual reference [1]); single differential (SD); double differential (DD); Laplacian (NDD).

The algorithm was implemented in Matlab and tested on the three following personal computers (acquired between 5 and 2 years ago), in order to investigate the time required to process an epoch:

- PC1: Intel(R) Dual-Core, T5500, with clock frequency 1.66 GHz, 2 GB of RAM, 32 bits operating system;
- PC2: Pentium(R) Dual-Core, with clock frequency of 2.8 GHz, 4 GB of RAM, 64 bits operating system;
- PC3: Intel(R) Core i7-2630QM, Quad-Core, with clock frequency of 2 GHz, 6 GB of RAM, 64 bits operating system.

2.2.2 Example of application: identification of patterns of co-contractions

Monopolar interference surface EMGs were simulated using the same simulator described in Section 2.2.1. Four different muscles were simulated (muscle geometry is represented in Figure 8A). They had rectangular cross-sections with 30 mm of lateral extension and were either superficial (maximal depth lower than 8 mm) or deep (range of depth between 9 and 16 mm). The muscle fibres were 200 mm long, with two IZs uniformly distributed among the MUs of the muscles and located 20 mm apart from each other. An interference signal (20 s in duration, force level 75% MVC) was simulated for each muscle as recorded by electrode grids covering the same portion of muscle (centred half way between the tendons, with dimension 50 mm along the fibres

and 100 mm in the transverse direction) with different densities: IED between 5 and 10 mm were considered. The basis waveforms simulated sources with 6 possible depths (between 1 and 16 mm), 11 transversal distances (between -50 and 50 mm) and either of the 2 IZs: thus, a total number of 132 waveforms were simulated (notice that, having 2 randomly distributed IZs implies that the number of waveforms, and thus also of unknowns, is doubled). It is worth noticing that the number of electrodes was larger than the number of basis waveforms only for IED = 5 mm and the investigated mathematical problem was over-determined only in such a case. The algorithm was first applied to 5 s of each of the 4 signals simulating the selective contraction of a single muscle: the distribution of sources was computed for each 50 ms epoch and then averaged to estimate the mean distribution associated to the activity of each muscle. This phase was a sort of training of the algorithm, which learned the distribution associated to the activity of each of the 4 investigated muscles. Then, the signals of different muscles were summed in order to simulate all the 15 possible co-contractions (4 single muscle contractions plus 6 pairs of co-contracting muscles plus 4 triplets and 1 case in which all muscles were co-contracted). The algorithm was tested on these 15 patterns of activations, considering epochs of 50-200 ms. The estimated distribution was decomposed in the least mean squares sense as a linear combination of the 4 distributions associated to the selective activation of each of the 4 muscles. The rational of this decomposition is that the distribution estimated from the activity of the muscles is well approximated by the sum of the distributions obtained processing the activation of each muscle separately (correlation coefficient above 98%). Indeed, the contribution of each source is linearly combined in the recorded signal. Moreover, the algorithm requires mostly linear operations, with the exception of the imposition of the positivity constraint. This property allows to identify the contribution in a co-contraction of each of the considered muscles.

3. Results

Figure 1 shows the simulation model, indicating the geometry and the conductivity of the volume conductor, the anatomy and position of the considered MUs. The active region changes during the

simulation. As a consequence, the simulated interference signal shows variations in amplitude, both in time and across different channels.

Figure 2 shows an example of application of the algorithm. Each epoch of EMG is approximated as a sum of amplitude scaled and delayed basis waveforms, each representing the activity of a specific region within the muscle. Four sample epochs are selected in Fig. 2A and considered in Fig. 2B. The distribution of activities was computed for each considered time sample. Such a distribution was then cumulated over the delays obtaining the average activity of each region within the muscle in the considered epoch (the contour plot of the distribution is shown for each of the four selected epochs in Fig. 2B). The barycentre of the distribution is computed and compared with that of the centres of the MUs which are active in the considered time epoch (the locations of the MUs which fire during the epoch are shown in Fig. 2B). Repeating this estimation for each epoch in which the simulated signal is divided, the performance of the method can be assessed (the estimation of depth and transverse displacement are shown in Fig. 2C).

Figure 3 considers different errors in the anatomy of the muscle or in the geometrical or conductivity properties of the model used to generate the basis waveforms: A) skin thickness, B) fat thickness, C) skin conductivity, D) muscle conductivity, E) fibre length, F) IZ location. A mistake in the thickness of the tissues over the muscle determines a bias in estimating the depth of the active region. The variation of distance of the detection system from the sources determined by a wrong measurement of the thickness of the tissues is in part ascribed by the algorithm to the depth within the muscle (e.g., if the fat layer is assumed to be thinner, the estimated depth within the muscle is larger). However, the relative depth within the muscle is still kept. Consider also that, using an ultrasound or MRI system, the measurement of the tissue thickness is expected to be more precise than the simulated conditions.

It is noteworthy that the estimation is not much affected, neither by the skin conductivity (which could have large variations both between and within subjects during an experiment), nor by the muscle conductivity (which is not simple to measure).

There is a bias in the estimation of the superficial active regions when too short fibres are used to simulate the basis waveforms, a bias in estimating the deep active regions if the basis waveforms refer to fibres which are too long. This is probably due to the contribution of non-propagating, end-of-fibre components: if the fibres are assumed short, the basis waveforms have a higher content of such components, biasing the location of superficial active regions, which have a low content of end-of-fibre components; vice versa if the fibres are assumed too long.

The performances are largely affected by an error in locating the IZ. The simulated conditions consider a maximal displacement which is larger than the IED. The localization of the IZ from HDsEMG can be very precise [7]. However, the IZ can move under the electrode grid (both in isometric [37][38] and in dynamic contractions [39]). In such a case, different kernel matrices could be saved for different locations of the IZ and selected, e.g., on the basis of the measured joint angle. As an alternative, the electrodes could be placed between the IZ and a tendon, being careful that the IZ does not shift under the electrodes during the investigated movement. This could be useful also to record less correlated information (some of the simulated channels on either side of the IZ record the same potentials).

Figure 4 considers A) different spatial filters or possible problems related to B) misalignment of the detection system with respect to the fibres, C) experimental noise, D) CV.

The performances of the method decrease as the spatial filter is more and more selective. Indeed, the detection volume is smaller for more selective spatial filters. The performances are only slightly degraded when using the monopolar detection with virtual reference. Thus, this detection method could be used instead of other spatial filters in cases in which large non-physiological CM components corrupt the signal.

The error in locating the depth of the active region is largely affected (mostly in the superficial region) by a possible misalignment of the electrode grid, when it is about 10° or higher. Indeed, a misalignment with respect to the fibres induces large variations of the shapes of the action potentials in the channels that the algorithm assumes to be aligned to the muscle fibres. Thus, the

EMG cannot be represented accurately by model (1) and the estimated activity distribution is not reliable. Hence, care should be given in placing the electrode grid (or in estimating the misalignment, if the muscle has not parallel fibres [40][41]; in such a case, the misalignment should be considered in simulating the basis waveforms). Another possible way to counteract misalignment problems is to reduce the number of channels aligned to the fibres and increase the density of the channels in the transverse direction. This solution could be a strict requirement, e.g. in the cases in which the fibres change orientation in different dynamic tasks of the investigated muscle.

The effect of noise is clearly visible when the SNR is about 15 dB or lower. The most affected are the deepest active regions, as they are associated to a smaller EMG with respect to the superficial ones.

There is a bias toward lower depths if a larger CV is considered and toward higher depths if the CV used to simulate the basis waveforms is smaller than the average CV of the simulated MUs. This result could be interpreted considering that a larger CV corresponds to a larger contribution of the high frequency components in the spectrum [42]; a large contribution of high frequency components in the EMG is also obtained when superficial MUs are active (vice versa, in the case of small CV, the spectrum is scaled toward the low frequency components [42], as if the active region was deep in the muscle).

Figure 5 shows the results of the whole tests, considering three different durations of the processed epochs (50, 100 and 150 ms) and all the testing conditions shown in Figures 3 and 4. The results are shown in terms of mean and standard error (to make the figure more readable with respect to using the standard deviation, as in Figures 3 and 4; note that the number of epochs is larger when they are shorter, reducing the standard error). We can notice that the mean error is always lower (with very few exceptions) when the duration of the epoch is larger. A further additional result is shown in panel I), where the compensation of CV is considered: the error is slightly reduced when the average CV is equal to that used in the model simulating the basis waveforms, suggesting that the compensation is not needed if the simulated CV is the same as the average CV of the MUs (the

variations within different epochs, due to the random recruitment of MUs with simulated Gaussian distributed CV, can be neglected); the reduction of the error by CV compensation is very important when the average CV varies of about 10-20% with respect to the simulated one (with larger reduction in the case in which the CV used for the basis waveforms is lower than the average value of the simulated MUs).

In Figure 6, the mean estimation error in localizing the sources was computed considering 300 different simulations of the basis waveforms, obtained choosing the following parameters randomly (Gaussian distribution, with mean given by the correct value and standard deviation specified below): skin thickness, fat thickness, skin conductivity, muscle conductivity (standard deviation of the previous 4 parameters equal to the 30% of the correct value), IZ displacement (standard deviation 3 mm), fibre length (standard deviation equal to the 10% of the correct value), angle of misalignment (standard deviation of 5°) and CV (standard deviation equal to 0.4 m/s). Considering a random choice of the parameters allows to make a test closer to the experimental conditions, in which different parameters can be estimated within some degree of accuracy. The possible variations of the parameters were chosen within reasonable ranges, considering the accuracy with which the thicknesses of tissues could be estimated (about 1 mm), the possible error in the conductivity of the tissues, the error in estimating the position of the IZ (about 5 mm) or the length of the fibres (about 1 cm), the misalignment of the electrode grid with respect to the fibres (up to about 10°) and the mean CV (that could vary during the contraction). Moreover, a white Gaussian noise was added with SNR of 20 dB. The localization errors are in the range 1-2.8 mm. The results are in line with the sensitivity analysis performed before. For example, the accuracy of the estimation is not largely affected neither by a reasonable mistake in the thickness of the skin or fat layer, nor by an error in the conductivity of the tissues used in the model simulating the basis waveforms: in the first 4 upper panels, the points indicating the mean error in different tests form a cloud which is hard to be interpolated with a second order polynomial. The mean error is affected by a displacement of the IZ: the errors increase in the average when a displacement of IZ affected

the generation of the basis waveforms. The mean error is marginally affected by a mistake in the estimation of the fibre length: indeed, the errors in different simulations are quite grouped about the interpolating parabola, which has a minimum close to the correct value of 100 mm. The error is largely affected by a misalignment: in this case, the error points follow quite well the interpolating parabola (apart from some outliers), which is symmetric with a minimum around 0°. The mean error is also affected by CV: the error points are quite clustered around the interpolating parabola, which has a minimum on the right (in line with the sensitivity analysis shown in Figure 5, where the error obtained using a CV of 4.5 was lower than that obtained using a CV of 3.5 m/s).

Figure 7 shows the processing time (mean and standard deviation) of the reference processing (but equivalent results are obtained for all other cases discussed above), considering different durations of the epochs and including or excluding the CV compensation (which requires to find the electrode array with maximum amplitude, to estimate CV and to rescale each channel accordingly). The computational cost is increasing at a rate which is about quadratic. Notice that the number of unknowns increases with the epoch duration with a rate which is less than linear (the number of unknowns is about equal to the number of measurements for short epochs of a few tenths of ms, whereas it is about a half of the number of measurements for long epochs of hundreds of ms). Thus, the dimension of the matrixes involved in the method increases at a rate which is less than quadratic. Moreover, the algorithm requires only products of square matrixes with vectors which has a cost of about N^2 (where N is the number of measurements). Using the first two PCs, the processing time is longer than the duration of the processed epoch. Moreover, the first PC failed to process epochs of 150 ms, for memory problems. The third PC has a processing time lower than the duration of the epoch if the CV compensation is excluded and if the epoch duration is as long as 200 ms. For epochs longer than 300 ms, memory problems occurred. However, in order to reduce the computational cost, a long epoch could be decomposed into a set of smaller ones (being careful to include at least a few complete MUAPs, i.e. using epochs of at least 10-20 ms). Consider also that in many applications (e.g., prosthesis control or biofeedback), using epochs of duration longer

than 100 ms could be detrimental, as a long delay would be introduced (for example, delays up to 100 ms are considered as tolerable in prosthesis control [43]; such a delay includes the time needed to record and process the signal, including also the post-processing necessary to choose the control command). Finally, a note on CV compensation: most of the time is spent to rescale the signals from all the channels. As the compensation of CV is really useful only if the variations are in the order of 10% or larger (refer to Figure 4D), in case of large CV variations (induced by different contraction levels [31] or fatigue [32]), it is suggested to save more kernel matrixes, each corresponding to a certain average CV (e.g., 3.5, 4.0, 4.5 m/s) and to monitor CV occasionally to select the proper matrix.

Figure 8 and Table 1 show the results of the application of the algorithm to the identification of different patterns of co-activation of 4 muscles. Two muscles are superficial and two are deep (Figure 8A). Two muscles (M2 and M3) are one over the other. By symmetry, the co-activation of M1 and M4 is equivalent to that of a muscle placed over M4 and another located under M1: thus, the simulated conditions could be extended to the case in which there are 3 superficial and 3 deep muscles. Similar muscle distributions are found in the human body: for example, in the forearm, the muscles extensor carpi radialis, extensor digitorum communis and the extensor carpi ulnaris are superficial and are placed over the supinator muscle; in the leg, the vastus medialis, rectus femuris and vastus lateralis are superficial muscles and the vastus intermedius is a deep one (placed under the rectus femuris). Two IZs were randomly distributed in the simulated muscles. Figure 8B shows an examples of simulated signal, where waveforms propagating in different directions are visible (due to the two IZs). The algorithm was first applied to 5 s of EMGs resulting from each of the selective contractions of the muscles: Figure 8C shows the mean distributions associated to each muscle. Notice that the activity of deeper muscles results in a lower amplitude of the estimated distribution, due to the normalization of the waveforms (used to consider a constant regularization parameter without introduce a bias with respect to depth [19]). The results of the identification of the co-activations are reported in Table 1. The performances increase for longer epochs (the mean

correct classification rate was 94.8 and 96.7% for epoch durations of 50 and 200 ms, respectively[1]). Performances were not degraded by a lower electrode density. The classification errors were mostly related to a problem in identifying the level of activity of the deep muscle M3 (probably due to the blurring of the estimated distribution associated to the activity of M2, which is placed over M3).

Table 1. Results of the test on the identification of muscle co-activation. Correct classifications are indicated as a percentage of the total test epochs.

Active muscles					Percentage of correct identifications			Most common error
					IED 5 mm	IED 7.5 mm	IED 10 mm	
					Epoch duration (ms)			
					50 |100|150|200	50 |100|150|200	50 |100|150|200	
1	M1				100|100|100|100%	100|100|100|100%	100|100|100|100%	
2		M2			100|100|100|100%	99|100|100|100%	100|100|100|100%	
3			M3		100|100|100|100%	100|100|100|100%	100|100|100|100%	
4				M4	100|100|100|100%	100|100|100|100%	100|100|100|100%	
5	M1	M2			100|100|100|100%	100|100|100|100%	100|100|100|100%	
6	M1		M3		70| 76| 79| 80%	80| 84| 87| 86%	93| 95| 95| 96%	6→1
7	M1			M4	100|100|100|100%	100|100|100|100%	100|100|100|100%	
8		M2	M3		100|100|100|100%	100|100|100|100%	100|100|100|100%	
9		M2		M4	91| 94| 95| 95%	79| 84| 86| 87%	77| 83| 84| 86%	9→14
10			M3	M4	100|100|100|100%	100|100|100|100%	100|100|100|100%	
11	M1	M2	M3		71| 76| 77| 79%	87| 92| 93| 93%	80| 88| 89| 91%	11→5
12	M1	M2		M4	79| 82| 84| 83%	78| 84| 86| 87%	95| 97| 98| 98%	12→5
13	M1		M3	M4	94| 97| 97| 97%	97| 98| 98|98%	100|100|100|100%	13→7
14		M2	M3	M4	100|100|100|100%	100|100|100|100%	100|100|100|100%	
15	M1	M2	M3	M4	97| 98| 98| 98%	99| 99| 99| 99%	100|100|100|100%	15→12

4. Discussion

Surface EMG found many important applications in the study of muscles, both in healthy and pathological conditions [4-6]. The estimation of the location of the active regions within a muscle was addressed only in a few works, probably due to the difficulty of the problem. Indeed, simulations clearly indicated the important effect of even small details in the conductivity or geometry of the volume conductor in the recorded potential [23][44-49]. Moreover, locating the sources of the recorded EMG is an inverse problem, affected by stability issues [13]. Thus, even small imprecisions in the representation of the volume conductor could result in large mistakes in the estimates. For this reason, regularization methods applied to detailed (MRI based) volume

[1] As expected, performances were even higher if the method was trained on 5 s of all 15 possible co-activations to be identified, instead of only on the selective activations of the 4 muscles. Mean correct classification rates were 98.8 and 99.4% for epochs of 50 and 200 ms, respectively.

conductor models have been recently proposed [19-20]. However, this approach has a high computational cost, precluding real time applications (discussed below), which could even benefit from a rough estimate. Thus, as a valuable alternative, this paper proposes an algorithm which provides approximate localization of the active regions in a muscle from HDsEMG in real time. Indeed, when it is run on a modern PC (with medium performances), it is fast enough to complete the computations in a time lower than the duration of the processed epoch of EMG (up to 200 ms of epoch duration). Faster processing could be obtained using a more efficient processor, a compiled routine (instead of the Matlab implementation here considered) or by separating the epoch into short adjacent portions and cumulating the estimated distributions (using shorter epochs, also the memory load is reduced). In this way, the time needed to record and process the shortest epoch here considered (which is 50 ms in duration) could be of about 60 ms (i.e., the epoch could be divided into portions of 10 ms, so that 50 ms are required to record the signal and process the first part and about 10 ms are needed to process the last portion). This time is close to the electromechanical delay in human skeletal muscles (which is about 50 ms [50]).

The estimates provided by the algorithm are approximate as there is no attempt to identify single sources (as proposed in [19-20], where a regularized under-determined approach is used). An over-determined regularized problem is solved to approximate the recorded EMG as the linear combination of a set of basis waveforms, each representing the activation of a muscle region.

The method was tested on the basis of simulations, showing a sensitivity analysis and a representative example of application. The sensitivity analysis was performed considering a test condition in which a single muscle region was active in each time epoch. A specific detection system was considered which properly covered the muscle. Different perturbations of the test signal or of the basis waveforms were considered, to test the sensitivity of the estimates to experimental problems (related to noise or electrode placement) or to reasonable errors in replicating the anatomy of the muscle when simulating the basis waveforms. A plane layer model was used to simulate interference EMG from muscle fibres of finite length. The configuration of the detection system and

the regularization parameter were chosen after a fine tuning based on preliminary tests in which the basis waveforms were generated with the same simulator used for generating the test interference EMG. The selected condition guarantees to approximate well the investigated signal with a linear combination of the basis waveforms (with a root mean square error of about 2-3%). Different choices could better fit different applications, so that a preliminary study of the proper set of detection channels and basis waveforms is required. For example, the IED, the dimension of the electrodes, the number of rows and columns of the detection system may affect the accuracy of the estimates, depending on both the investigated muscle (in terms of location, dimension, anatomy) and task (e.g., the position of the IZ, the fibre length and their orientation could change during the specific contraction under study; in such a case, I suggest to place more channels in the transverse direction, far from the IZ, and only a few along the fibres, which are more affected by a variation of IZ displacement, fibre length or orientation).

The simulated active region was moved around the muscle, with a small change in the average depth (in the range 2-8 mm) and a larger variation in the transverse direction (average location in the range -30 to 30 mm, with respect to the centre of the 2D detection grid). As expected, locating the transverse location was very simple. Thus, identifying the activity of different muscles located at different locations under the skin (like biceps and triceps, investigated by an array placed around the upper arm [19-20]) is not difficult. On the other hand, problems were found in identifying the depth of the active regions.

The best results were obtained considering monopolar detections, in line with the conclusions of [19]. Indeed, the monopolar signal has a larger detection volume than that of other spatial filters, which were designed to be selective to the activity of a specific (usually superficial) region of the muscle [2]. Using the virtual reference for monopolar detection determined a small degradation of the results: indeed, such a derivation removes the CM of the signal, largely affecting generation and extinction components, which are far field potentials, providing contributions even from deep muscle regions. Thus, this result is not surprising, as both propagating and non-propagating

components (taken separately or considering their relative weights) provide useful information to estimate the location of the active regions within a muscle. By using more selective filters (SD, DD, NDD), the localization of the sources is increasingly degraded (as selective filters remove the CM components and have a small detection volume, which exclude the deep sources).

An error in the simulation of the basis waveforms used to approximate the EMG reflected in a mistake in the localization of the sources. The sensitivity of the method to errors in the basis waveforms was assessed, with the following indications.

1. An error in the estimation of the thickness of subcutaneous layers determines a bias in the location of the active regions, but relative depth information is preserved.
2. If fibres are longer or shorter than expected, there is a bias toward the deep or superficial portions, respectively, due to the erroneous evaluation of the end-of-fibre components.
3. If the IZ is displaced in the basis waveforms, there is a bias in the estimation toward the deep direction.
4. The effect of a mistake in the conductivity of the tissues is marginal.
5. An error in CV has important effects only if it is at least as large as 10% of the average correct value.
6. A misalignment of about 10° between the electrodes and the muscle fibres determines a bias in the estimation of the superficial sources. Care should be taken in placing the electrodes or the misalignment should be considered in generating the basis waveforms (especially for muscles with different fibre directions [40][41][48]).

Moreover, tests with the presence of additive noise were performed: the noise reduces the ability of the method to localize deep sources, especially when the SNR is lower than 15 dB.

In general, the sensitivity analysis indicated that the method can provide stable information, with errors in the estimation of the average depth of an active region of the order of 1.2 mm, if the volume conductor is well represented in the generation of the basis waveforms. Some bias is present if the assumed volume conductor used to build the basis waveforms is different from the actual

tissue investigated. For example, when the basis waveforms were generated using a model with parameters randomly chosen about their correct values, the average estimation errors were in the range 1-2.8 mm. However, if the basis waveforms do not provide an accurate representation of the activity of the muscle, the approximation of the interference signal provided by the method is poor, indicating that they should be refined. Consider also that, even in the presence of a bias, relative information about the location of the active regions can be obtained. A more important problem could be encountered in the case of non-stationary conditions, changing the shapes of the MUAPs: for example, this happens in the presence of large CV variations or in dynamic conditions. In such cases, the physiological system can be periodically monitored and different basis waveforms (e.g., associated to different CV or representing a different IZ location or shortening of the fibres) can be selected, in order to better represent the actual conditions.

A further representative test on simulation was performed to investigate the performance of the algorithm in identifying the co-activation of different nearby muscles. The simulated conditions were complicated by the presence of two different IZs, randomly distributed in the muscles, which required to simulate more waveforms to represent their effect. Moreover, different densities of the electrode grid were considered and only with the largest one (with IED = 5 mm) the problem was over-determined. The source distributions estimated from EMG during co-activation of different muscles were approximately equal to the sum of the source distributions computed processing the selective activation of each muscle separately. This property allowed to identify different patterns of co-activation after decomposing the estimated source distribution as a linear combination of the distributions related to the selective contraction of each muscle. The identification of the co-contraction pattern was quite accurate, even using short epochs and low electrode density (showing that, for this specific application, useful indications can be obtained even considering an under-determined problem).

Estimating the location of the active region within a muscle or investigating the co-activation of different muscles could be useful to address many interesting problems.

1. The diagnosis of musculoskeletal deficits, as a problem in assessing a specific portion of the muscle could be assessed.
2. Guiding rehabilitation, indicating activity variations in individual muscles (instead of limiting to a functional assessment [51]).
3. The investigation of muscle synergies [52][53], by assessing the muscles (or portions of muscles) with synergic activity during a specific movement.
4. Reducing cross-talk [54][55], as the signal of the nearby muscles could be identified, estimated and subtracted [20].
5. Different tasks or torque directions could be accomplished using the same muscle, but activating different regions [56][57]. Identifying the active region within a muscle could be important to investigate the different functional properties of the same muscle performing different tasks.
6. Different nearby muscles can be involved in different tasks with a different weight. Identifying the location of the sources, the level of activation of each muscle could be investigated [19]. This could be useful to identify the task on the basis of the surface EMG (e.g., for the control of a prosthesis [20]) or to investigate the load sharing among synergic muscles [58].
7. Different portions of a muscle could be recruited or de-recruited/refreshed during an endurance task [59][60]. Identifying the active regions, the control strategy during a fatiguing task could be addressed.
8. Many methods for force estimation from surface EMG are based on the envelope of the recorded signal [61]. The estimation of the location of the active regions could be used to estimate directly the force or to compensate for the effect on EMG amplitude of the distance from the sources to the detection channels.
9. The clinical assessment of motor axonal loss is usually quantified by the motor unit number estimation (MUNE), which is based on the ratio between the amplitude of the maximal

compound muscle action potential (CMAP) and that of the average single MU [62]. The localization of the sources could allow to compensate for the effect of their relative position with respect to the detection channel, in order to obtain a more accurate estimation of the average CMAP and MUAP.

Some of these potential applications require a real time processing and may tolerate a rough estimate. For example, prosthesis control [63] or rehabilitation with a biofeedback [64] would benefit on the localization of the active portions of the muscles only if the estimation is real time. Moreover, real time algorithms which require to reduce the effect of cross-talk (e.g., to provide biofeedback on force or fatigue) could benefit from the presented method. For example, consider a system which requires to estimate muscle fibre CV in real time from a muscle affected by cross-talk. Such a system could consist in a biofeedback providing the subject with information on fatigue, measured in terms of CV variations [32]. Otherwise, the system could be devoted to the control of a prosthesis or of an electrical stimulator (adapting the stimulation parameters to the myoelectric manifestations of fatigue [57]). The real time estimation of the active regions could be used to remove cross-talk as a pre-processing step before the estimation of CV, in order to get selective information on the specific investigated muscle.

The algorithm is here tested on simulations from a basic EMG model. Experimental data are represented only within some approximation by the considered simulations. However, as the proposed method provides approximate estimations, using a sophisticated simulator to test it on a specific inhomogeneity would not add much information. Moreover, the algorithm is adaptive, so that a specific inhomogeneity could be counteracted by the off-line investigation of the volume conductor and selection of the basis waveforms (which can be optimized till the EMG signal is well represented as a linear combination of the waveforms). An experimental test is not simple and beyond the aims of this paper. Indeed, the positions of the sources are difficult to measure. An attempt could be made by jointly recording the needle and the surface EMG. However, this is an invasive method, requiring to use many needles to properly investigate different regions. A non-

invasive possibility is investigating the activity of muscle regions with ultrasounds [65] while recording the EMG with a system of electrodes transparent to ultrasounds [22]. Also in this case, the resolution of the identification of the muscle activity could be a limitation. As an alternative, indirect indications of the value of the proposed method could be obtained by using the estimated distribution of activity to improve the performance of other algorithms, e.g. a movement classifier, a force estimator or a technique for CV estimation from signals affected by cross-talk. In such cases, a possible improvement of the stability and correctness of the estimates of the movements or of the developed force or a reduction of the bias on CV estimation during the activation of the nearby muscles would indicate the reliability and the value of the proposed method. Such tests are suggested for further future works.

6. Conclusions

This paper proposes an innovative, real time method for the localization of the muscle sources from HDsEMG. The method provides accurate estimates of the mean location of the sources of activity and is stable to possible detection problems or inaccurate knowledge of the anatomical or physical properties of the investigated tissues. The algorithm provides estimates in real time, opening potential future applications for prosthesis control or biofeedback.

REFERENCES

[1] R. Merletti, M. Aventaggiato, A. Botter, A. Holobar, H. Marateb, T.M. Vieira, Advances in surface EMG: recent progress in detection and processing techniques, Crit Rev Biomed Eng. 38 (2010) 305-345

[2] R. Merletti, A. Holobar, D. Farina, Analysis of motor units with high-density surface electromyography, J. Electromyography, Kinesiol. 18 (2008) 879-890

[3] A. Holobar, M.A. Minetto, D. Farina, Accurate identification of motor unit discharge patterns from high-density surface EMG and validation with a novel signal-based performance metric, J. Neural Eng. 11 (2014) 016008.

[4] G. Drost, D.F. Stegeman, B.G.M. van Engelen, M.J. Zwarts, Clinical applications of high-density surface EMG: A systematic review, J Electromyogr Kinesiol., 16 (2006) 586–602

[5] R. Merletti, A. Botter, C. Cescon, M.A. Minetto, T.M. Vieira, Advances in surface EMG: recent progress in clinical research applications, Crit Rev Biomed Eng. 38 (2010) 347-79

[6] D.F. Stegeman, B.U. Kleine, B.G. Lapatki, J.P. van Dijk, High-density Surface EMG: Techniques and Applications at a Motor Unit Level, Biocybernetics, Biomedical Engineering, 32 (2012) 3–27

[7] N. Ostlund, B. Gerdle, S. Karlsson, Location of innervation zone determined with multichannel surface electromyography using an optical flow technique, J Electromyogr Kinesiol. 17 (2007) 549-55.

[8] R. Merletti, D. Farina, M. Gazzoni, The linear electrode array: a useful tool with many applications, J. Electromyogr. Kinesiol. 13 (2003) 37–47

[9] L. Mesin, A.K.R. Kandoor, R. Merletti, Separation of propagating and non-propagating components in surface EMG, Biomedical Signal Processing and Control, 3 (2008) 126-137

[10] L. Mesin, M. Gazzoni, R. Merletti, Automatic localisation of innervation zones: a simulation study of the external anal sphincter, J. Electromyogr. Kinesiol. 19 (2009) e413-e421

[11] A. Gallina, R. Merletti, M. Gazzoni, Innervation zone of the vastus medialis muscle: position and effect on surface EMG variables, Physiol Meas. 34 (2013) 1411-1422

[12] D. Farina, R. Merletti, Methods for estimating muscle fibre conduction velocity from surface electromyographic signals, Med Biol Eng Comput. 42 (2004) 432-45. Review. Erratum in: Med Biol Eng Comput. 42 (2004) 732

[13] C.M. Michel, M.M. Murray, G. Lantz, S. Gonzalez, L. Spinelli, R.G. de Peralta, EEG source imaging, Clinical neurophysiology, 115 (2004) 2195–2222

[14] E. Chauvet, O. Fokapu, D. Gamet, Inverse problem in the surface EMG: A feasibility study, in Proceedings of the 23rd Annual EMBS international Conference, Istanbul, Turkey (2001) 1048–1050

[15] R.A. Jesinger, V.L. Stonick, Processing signals from surface electrode arrays for noninvasive 3D mapping of muscle activity, in IEEE DSP Workshop Prodceedings (1994) 57–60

[16] E.F. LoPresti, R.A. Jesinger, V.L. Stonick, Identifying Significant Frequencies in Surface EMG Signals for Localization of Muscle Activity, in IEEE EMBS Conference Proceedings (1995) 967–968

[17] K. Roeleveld, D.F. Stegeman, H.M. Vingerhoets, A. van Oosterom, The motor unit potential distribution over the skin surface, its use in estimating the motor unit location, Acta Physiol. Scand. 161 (1997) 465–472

[18] J.T. Stonick, R.A. Jesinger, V.L. Stonick, S.B. Baumann, Estimation and localization of multiple dipole sources for noninvasive mapping of muscle activity, IEEE Proceedings of the International Conference on Acoustics, Speech, and Signal Processing, 5 (1996) 2912–2915

[19] K. van den Doel, U.M. Ascher, D.K. Pai, Source localization in electromyography using the inverse potential problem, Inverse Problems 27 (2011) 025008

[20] K. van den Doel, U.M. Ascher, D.K. Pai, Computed myography: three dimensional reconstruction of motor functions from surface EMG data, Inverse Probl. 24 (2008) 065010

[21] L. Mesin, A. Troiano, Motor unit distribution estimation by multichannel surface EMG, IEEE, MEDSIP (Advances in Medical, Signal, Information Processing) (2008) 1-3

[22] A. Botter, T.M. Vieira, I.D. Loram, R. Merletti, E. Hodson-Tole, A novel system of electrodes transparent to ultrasound for simultaneous detection of myoelectric activity and B-mode ultrasound images of skeletal muscles, J Appl Physiol. 115 (2013) 1203-1214

[23] M.M. Lowery, N.S. Stoykov, J.P. Dewald, T.A. Kuiken, Volume conduction in an anatomically based surface EMG model, IEEE Trans. Biomed. Eng. 51 (2004) 2138-2147

[24] S. Gabriel, R.W. Lau, C. Gabriel, The dielectric properties of biological tissues. 2. Measurements in the frequency range 10 Hz to 20 GHz, Phys. Med. Biol. 41 (1996) 2251–2269

[25] F.L.H. Gielen, W. Wallinga-de Jonge, K.L. Boon, Electrical-conductivity of skeletal-muscle tissue-experimental results from different muscles in vivo, Med. Biol. Eng. Comput. 22 (1984) 569–577

[26] D.W. Stashuk, Decomposition and quantitative analysis of clinical electromyographic signals, Med. Eng. Phys. 21 (1999) 389–404

[27] D. Farina, L. Arendt-Nielsen, R. Merletti, T. Graven-Nielsen, Assessment of single motor unit conduction velocity during sustained contractions of the tibialis anterior muscle with advanced spike triggered averaging, J. Neurosci. Methods, 115 (2002) 1–12

[28] L.C. Evans, Partial differential equations, Grad. Stud. Math., vol. 19, Amer. Math. Soc., Providence, Rhode Island, 1998.

[29] E.A. Clancy, E.L. Morin, R. Merletti, Sampling, noise-reduction and amplitude estimation issues in surface electromyography, J. Electromyogr. Kinesiol. 12 (2002) 1-16

[30] B. Johansson, T. Elfving, V. Kozlov, Y. Censor, G. Granlund, The application of an oblique-projected Landweber method to a model of supervised learning, Mathematical and Computer Modelling, 43 (2004) 892-909

[31] N. Hedayatpour, L. Arendt-Nielsen, D. Farina, Motor unit conduction velocity during sustained contraction of the vastus medialis muscle, Exp Brain Res. 180 (2007) 509-516

[32] L. Mesin, C. Cescon, M. Gazzoni, R. Merletti, A. Rainoldi, A bi-dimensional index for the selective assessment of myoelectric manifestations of peripheral and central muscle fatigue, J Electromyogr. Kinesiol. 19 (2009) 851–863

[33] D. Farina, W. Muhammad, E. Fortunato, O. Meste, R. Merletti, H. Rix, Estimation of single motor unit conduction velocity from surface electromyogram signals detected with linear electrode arrays, Med. Biol. Eng. Comput. 39 (2001) 225–236

[34] D. Farina, R. Merletti, A novel approach for precise simulation of the EMG signal detected by surface electrodes, IEEE Trans. Biomed. Eng. 48 (2001) 637-646

[35] A.J. Fuglevand, D.A. Winter, A.E. Patla, Models of recruitment and rate coding organization in motor-unit pools, J. Neurophysiol. 70 (1993) 2470–2488

[36] S. Andreassen, L. Arendt-Nielsen, Muscle fiber conduction velocity in motor units of the human anterior tibial muscle: A new size principle parameter, J. Physiol. 391 (1987) 561-571

[37] J.M. Defreitas, P.B. Costa, E.D. Ryan, T.J. Herda, J.T. Cramer, T.W. Beck, An examination of innervation zone movement with increases in isometric torque production, Clin. Neurophysiol., 119 (2008) 2795-2799

[38] H. Piitulainen, T. Rantalainen, V. Linnamo, P. Komi, J. Avela, Innervation zone shift at different levels of isometric contraction in the biceps brachii muscle, J. Electromyogr. Kinesiol., 19 (2009) 667-675

[39] K. Nishihara, H. Kawai, Y. Chiba, N. Kanemura, T. Gomi, Investigation of innervation zone shift with continuous dynamic muscle contraction, Comput. Math. Methods Med., 2013:174342 (2013)

[40] L. Mesin, Simulation of Surface EMG Signals for a Multi-layer Volume Conductor with Triangular Model of the Muscle Tissue, IEEE Trans. Biomed. Eng. 53 (2006) 2177-2184

[41] L. Mesin, D. Farina, Simulation of surface EMG signals generated by muscle tissues with in-homogeneity due to fiber pinnation, IEEE Trans. Biomed. Eng., 51 (2004) 1521-1529

[42] L. Lindstrom, R. Magnusson, Interpretation of myoelectric power spectra: A model and its applications, Proc. IEEE, 65 (1977) 653–662

[43] T.R. Farrell, R.F. Weir, The Optimal Controller Delay for Myoelectric Prostheses, IEEE Trans. Neural Sys Rehab Eng, 15 (2007) 111-118

[44] L. Mesin, M. Joubert, T. Hanekom, R. Merletti, D. Farina, A Finite Element Model for Describing the Effect of Muscle Shortening on Surface EMG, IEEE Trans. Biomed. Eng. 53 (2005) 593-600

[45] L. Mesin, D. Farina, A model for surface EMG generation in volume conductors with spherical inhomogeneities, IEEE Trans Biomed Eng. 52 (2005) 1984-1993

[46] L. Mesin, Simulation of Surface EMG Signals for a Multi-layer Volume Conductor with a Superficial Bone or Blood Vessel, IEEE Trans. Biomed. Eng., 55 (2008) 1647-1657

[47] J. Schneider, J. Silny, G. Rau, Influence of tissue inhomogeneities on noninvasive muscle fiber conduction velocity measurements investigated by physical, numerical modelling, IEEE Trans. Biomed. Eng. 38 (1991) 851-860

[48] L. Mesin, Volume conductor models in surface electromyography: Computational techniques, Comput. Biol. Med., 43 (2013) 942-952

[49] L. Mesin, Volume conductor models in surface electromyography: Applications to signal interpretation and algorithm test, Comput. Biol. Med., 43 (2013) 953-961

[50] P.R. Cavanagh, P.V. Komi, Electromechanical delay in human skeletal muscle under concentric and eccentric contractions. Eur J Appl Physiol Occup Physiol. 42 (1979) 159-163

[51] A. Curt, M.E. Schwab, V. Dietz, Providing the clinical basis for new interventional therapies: refined diagnosis and assessment of recovery after spinal cord injury, Spinal Cord. 42 (2004) 1–6

[52] E. Bizzi, V.C. Cheung, A. d'Avella, P. Saltiel, M. Tresch, Combining modules for movement, Brain Res Rev. 57 (2008) 125–133

[53] L. Gizzi, J.F. Nielsen, F. Felici, Y.P. Ivanenko, D. Farina, Impulses of activation but not motor modules are preserved in the locomotion of subacute stroke patients, J. Neurophysiol. 106 (2011) 202-210

[54] L. Mesin, S. Smith, S. Hugo, S. Viljoen, T. Hanekom, Effect of Spatial Filtering on Crosstalk Reduction in Surface EMG Recordings, Med. Eng. Phys. 31 (2009) 374-383

[55] J.M. Kilner, S.N. Baker, R.N. Lemon, A novel algorithm to remove electrical cross-talk between surface EMG recordings and its application to the measurement of short term synchronization in humans, The Journal of Physiology, 538 (2002) 919–930

[56] T.M. Vieira, I.D. Loram, S. Muceli, R. Merletti, D. Farina, Postural activation of the human medial gastrocnemius muscle: are the muscle units spatially localised? The Journal of Physiology, 589 (2011) 431-443

[57] J. Winslow, P.L. Jacobs, D. Tepavac, Fatigue compensation during FES using surface EMG, J Electromyogr. Kinesiol. 13 (2003) 555-568

[58] K. Bouillard, A. Nordez, P.W. Hodges, C. Cornu, F. Hug, Evidence of changes in load sharing during isometric elbow flexion with ramped torque, J. Biomech. 45 (2012) 1424-1429

[59] M.S. Stock, T.W. Beck, J.M. Defreitas, Effects of fatigue on motor unit firing rate versus recruitment threshold relationships, Muscle Nerve, 45 (2012) 100-109

[60] R.H. Westgaard, C.J. DeLuca, Motor unit substitution in long-duration contractions of the human trapezius muscle, J. Neurophysiol. 82 (1999) 501–504

[61] D.G. Lloyd, T.F. Besier, An EMG-driven musculoskeletal model to estimate muscle forces, knee joint moments in vivo. J. Biomech. 36 (2003) 765-776

[62] M.B. Bromberg, MUNIX and MUNE in ALS, Clin. Neurophysiol. 124 (2013) 433-434

[63] K. Manal, R.V. Gonzalez, D.G. Lloyd, T.S. Buchanan, A real-time EMG-driven virtual arm, Comput. Biol. Med. 32 (2002) 25-36

[64] J. Langenderfer, S. LaScalza, A. Mell, J.E. Carpenter, J.E. Kuhn, R.E. Hughes, An EMG-driven model of the upper extremity and estimation of long head biceps force, Comput Biol Med. 35 (2005) 25-39

[65] J. Darby, E.F. Hodson-Tole, N. Costen, I.D. Loram, Automated regional analysis of B-mode ultrasound images of skeletal muscle movement, J. Appl. Physiol. 112 (2012) 313–327

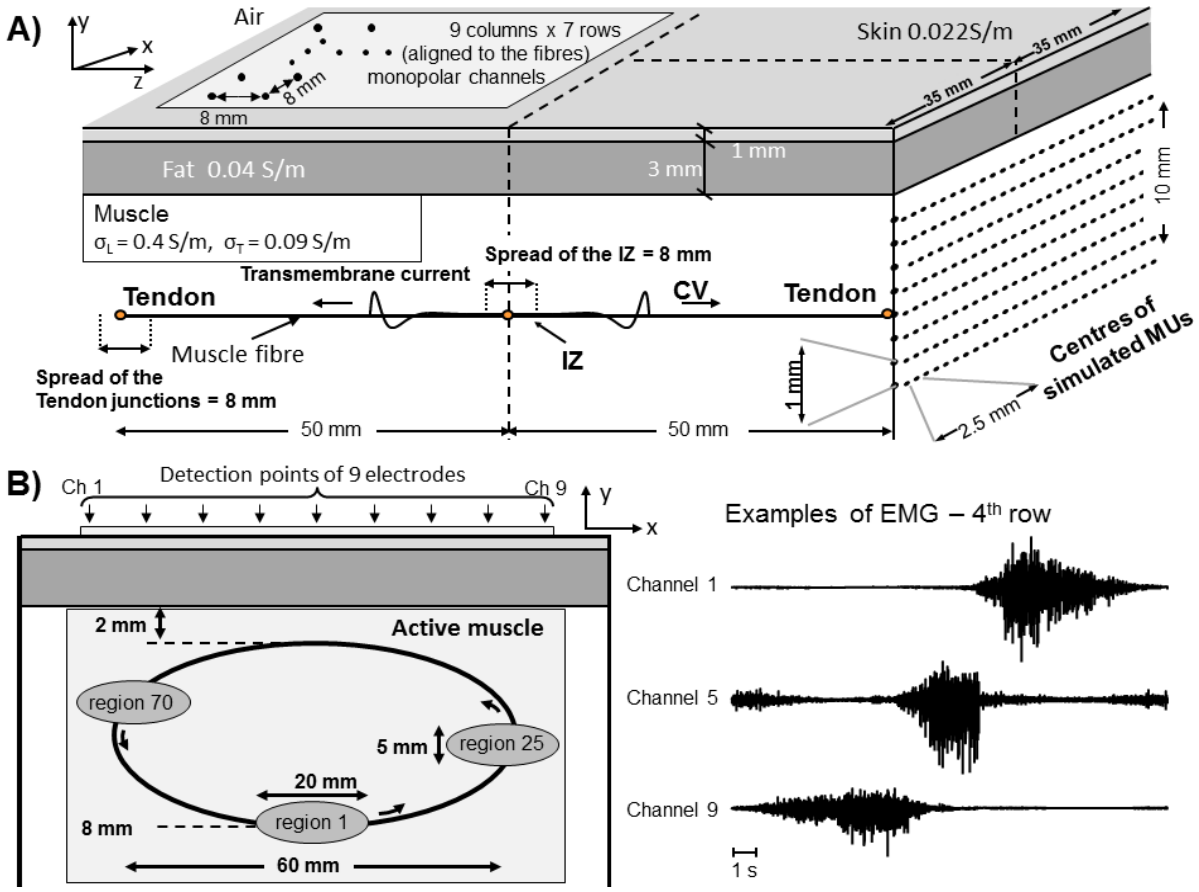

Figure 1. Description of the simulated interference EMG used for the sensitivity analysis of the algorithm. A) Plane layer volume conductor model, with indication of tissues thickness and conductivity, properties and location of the simulated muscle fibres (each corresponding to a motor unit - MU) and bi-dimensional detection grid of electrodes. B) Physiological cross-section area of the considered muscle (left), with a representation of the electrode grid, 3 of the 100 regions which are subsequently activated (small ellipses), and the path of the centres of the active regions (large ellipse); three monopolar EMGs are also shown (right).

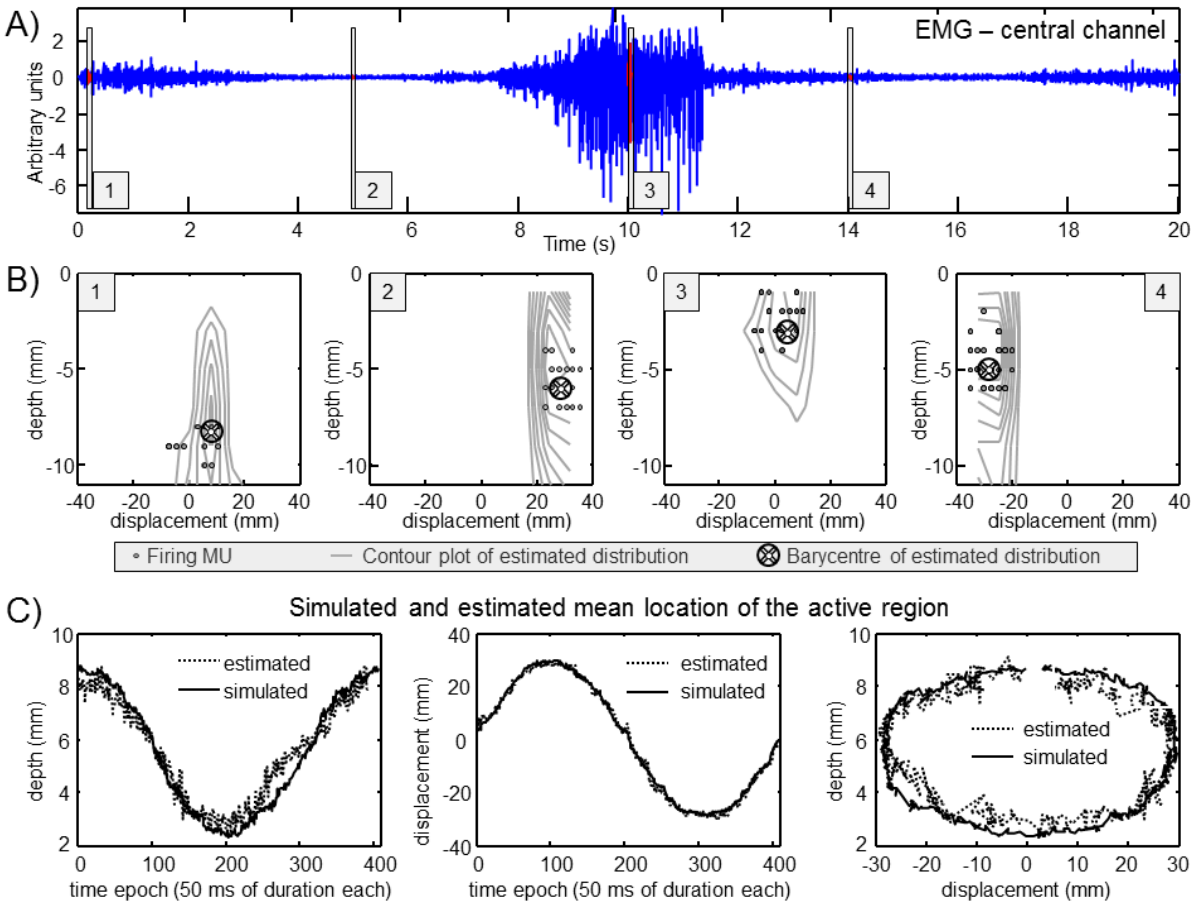

Figure 2. Representative example of application of the algorithm. A) Simulated monopolar interference EMG from the central channel (5th array, 4th electrode) and examples of four epochs (50 ms of duration) corresponding to four distinct active regions. B) Active MUs (firing at least one time within the epoch), contour plot and barycentre of the estimated activity distribution. C) Comparison between estimated and simulated location of the active region (from left to right: depth and transverse displacement, each across different epochs and together).

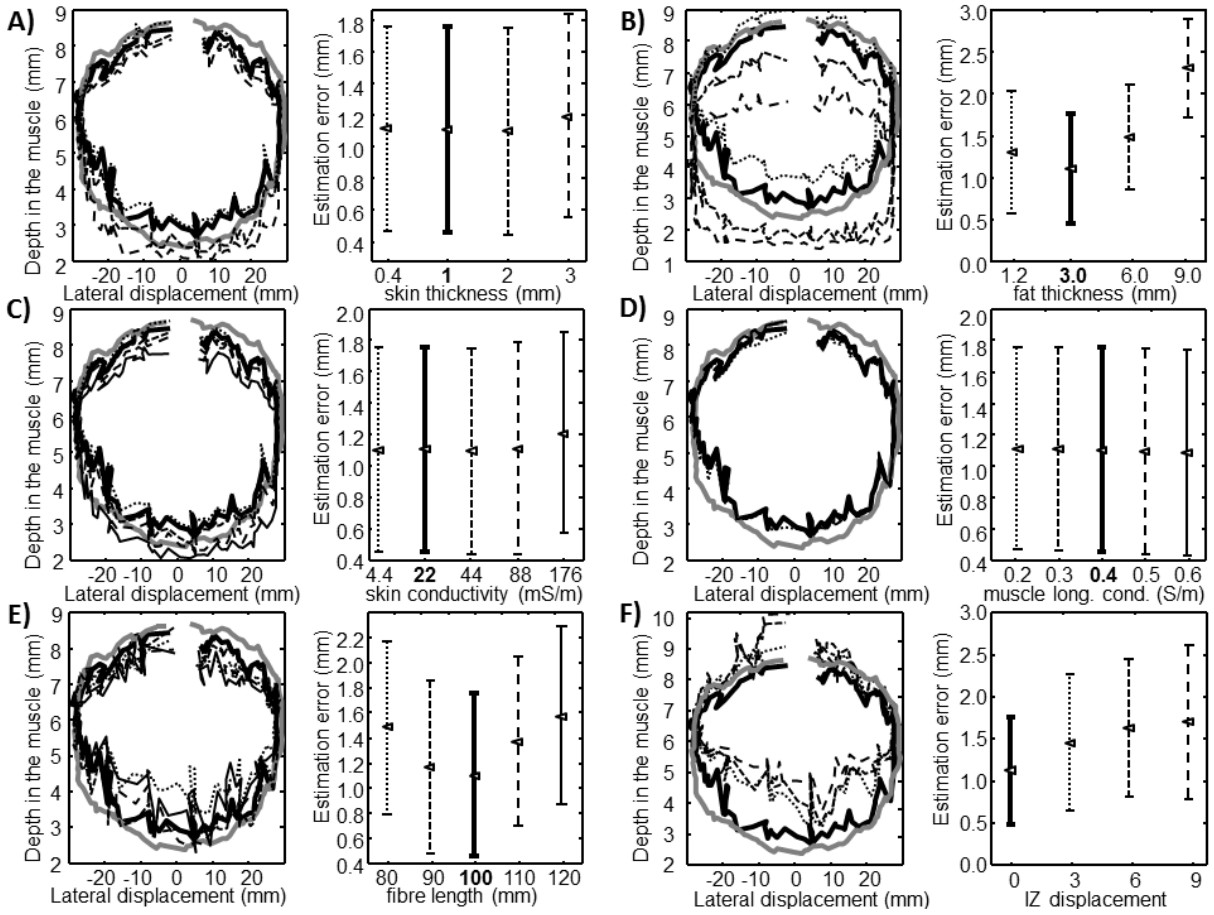

Figure 3. Sensitivity analysis when the simulation of the basis waveforms has problems in replicating the geometry or conductivity of the tissues or the anatomy of the muscle: A) skin thickness, B) fat thickness, C) skin conductivity, D) muscle conductivity, E) fibre length, F) IZ. In each panel, there are two graphs: the simulated (thick grey line) and estimated centre of the active region in non-overlapping epochs of 150 ms (left) and the estimation error (right; mean and standard deviation of the distance between simulated and estimated centre of the active region). The formats of the lines correspond in the two graphs (the thick, black line corresponds to the reference processing, using correct values of the parameters for the simulation of the basis waveforms).

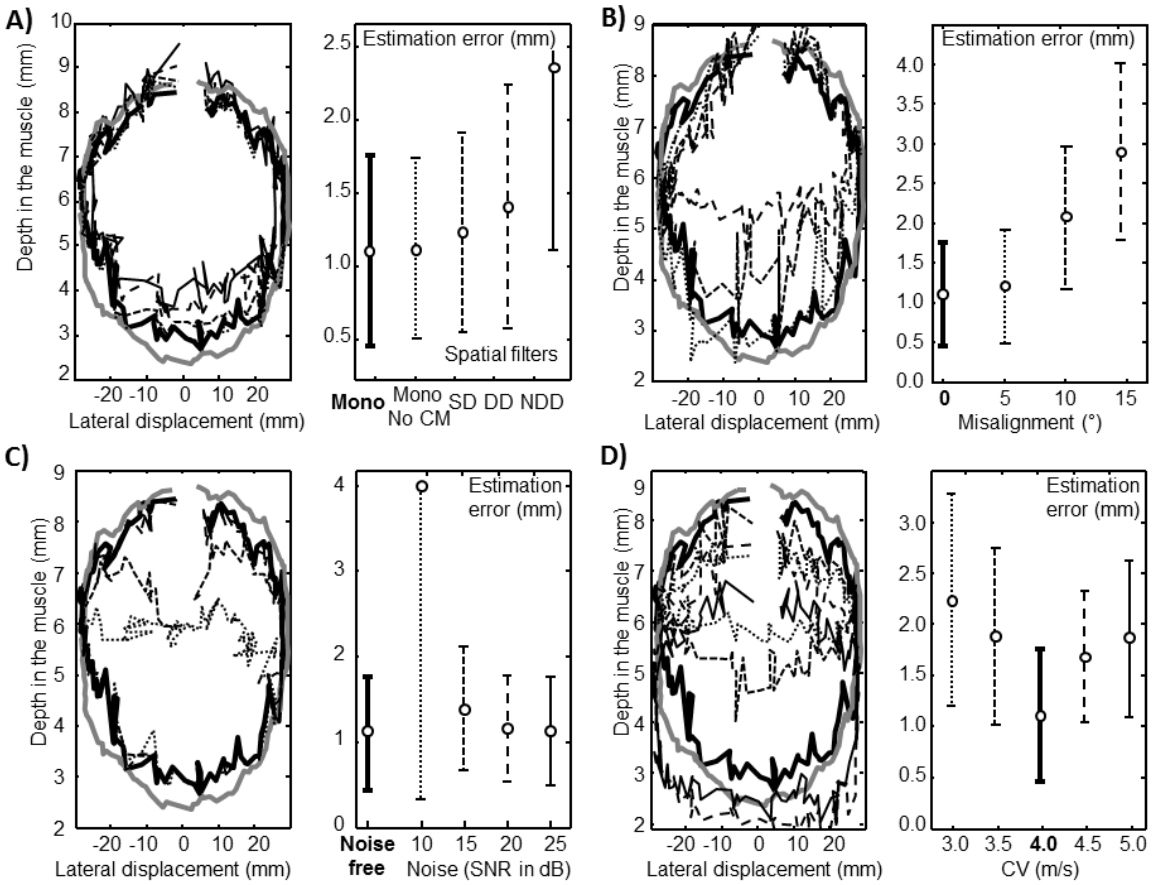

Figure 4. Sensitivity of the algorithm to the use of different spatial filters or to a bad orientation of the electrode array or to additive noise: A) spatial filters, B) misalignment of the detection system with respect to the fibres, C) noise , D) conduction velocity (CV). Same format as in Figure 3.

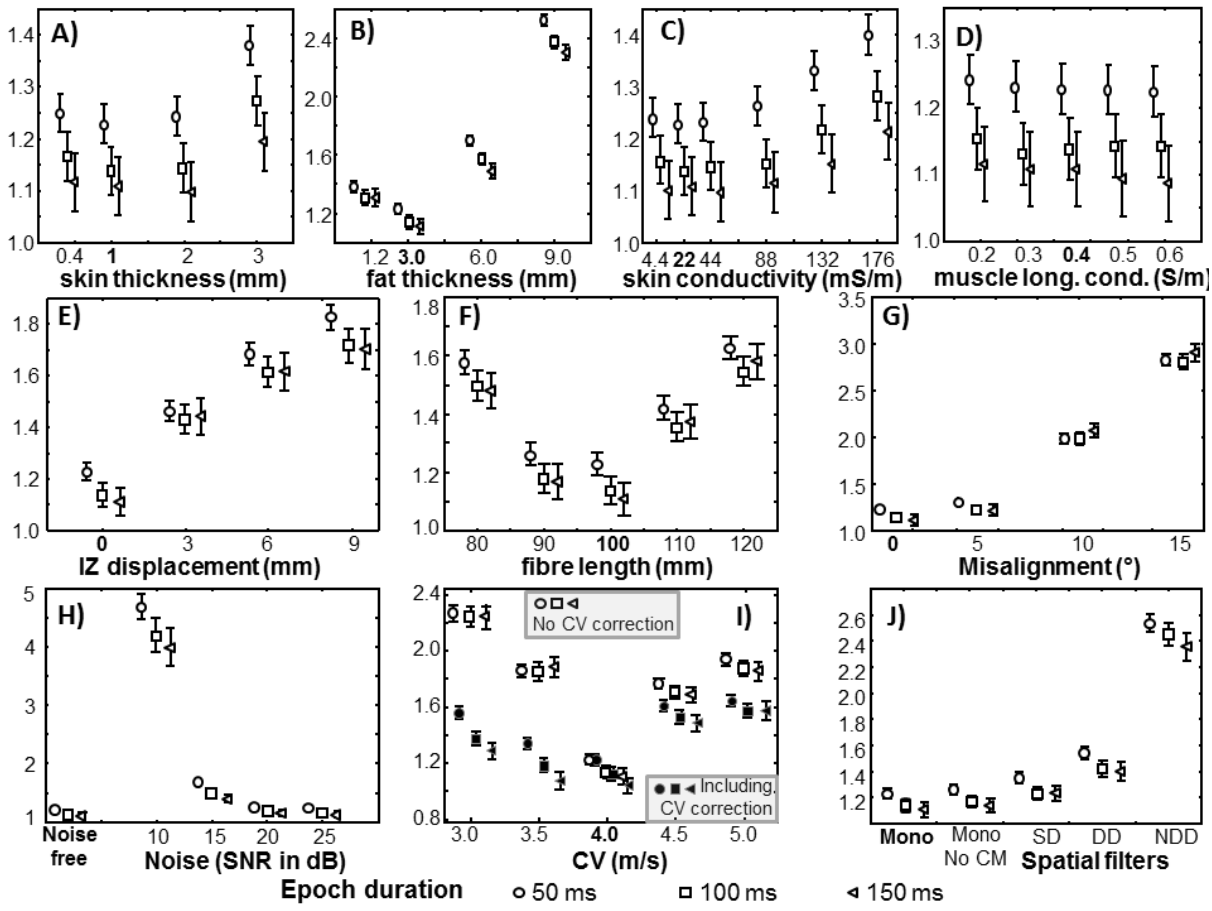

Figure 5. Collective results of the test of the algorithm (showing the mean and standard error of the distance between the simulated and estimated centre of the active region): A) skin thickness, B) fat thickness, C) skin conductivity, D) muscle conductivity, E) IZ displacement, F) fibre length, G) misalignment of the detection system, H) noise, I) conduction velocity (CV), J) spatial filters. Different epoch durations are considered. The bold label in each graph indicates the results of the reference condition (correct simulation parameters, monopolar noise free signals, short side of the detection matrix aligned to the muscle fibre).

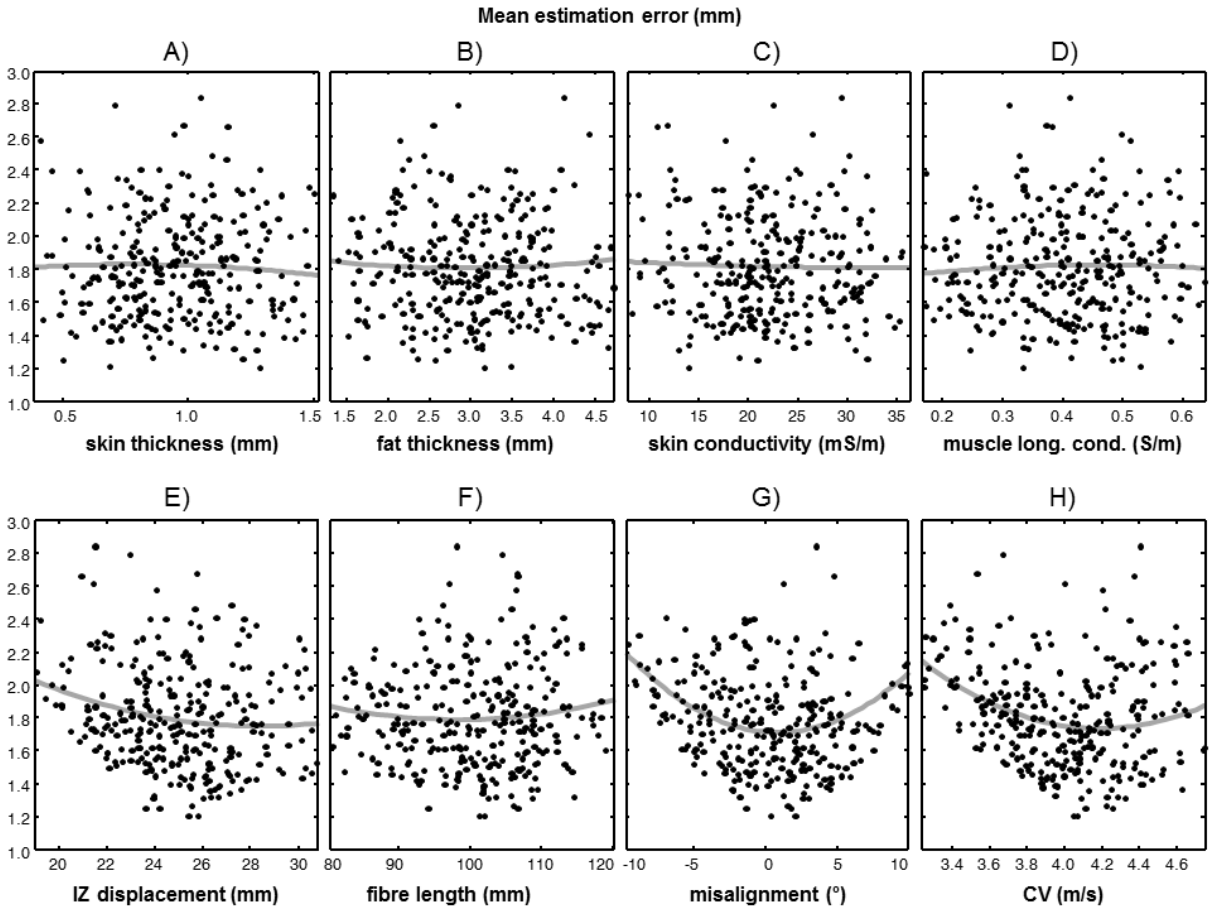

Figure 6. Mean error in the source localization obtained considering a noisy interference signal (SNR = 20 dB) and basis waveforms simulated using 300 different random choices of the following parameters: A) skin thickness, B) fat thickness, C) skin conductivity, D) muscle conductivity, E) IZ displacement, F) fibre length, G) angle of misalignment, H) conduction velocity. Monopolar signals were considered, with epochs of 150 ms. The mean error is shown as a function of each of the parameter at a time. The interpolation of the scattered points with a second order polynomial is also shown.

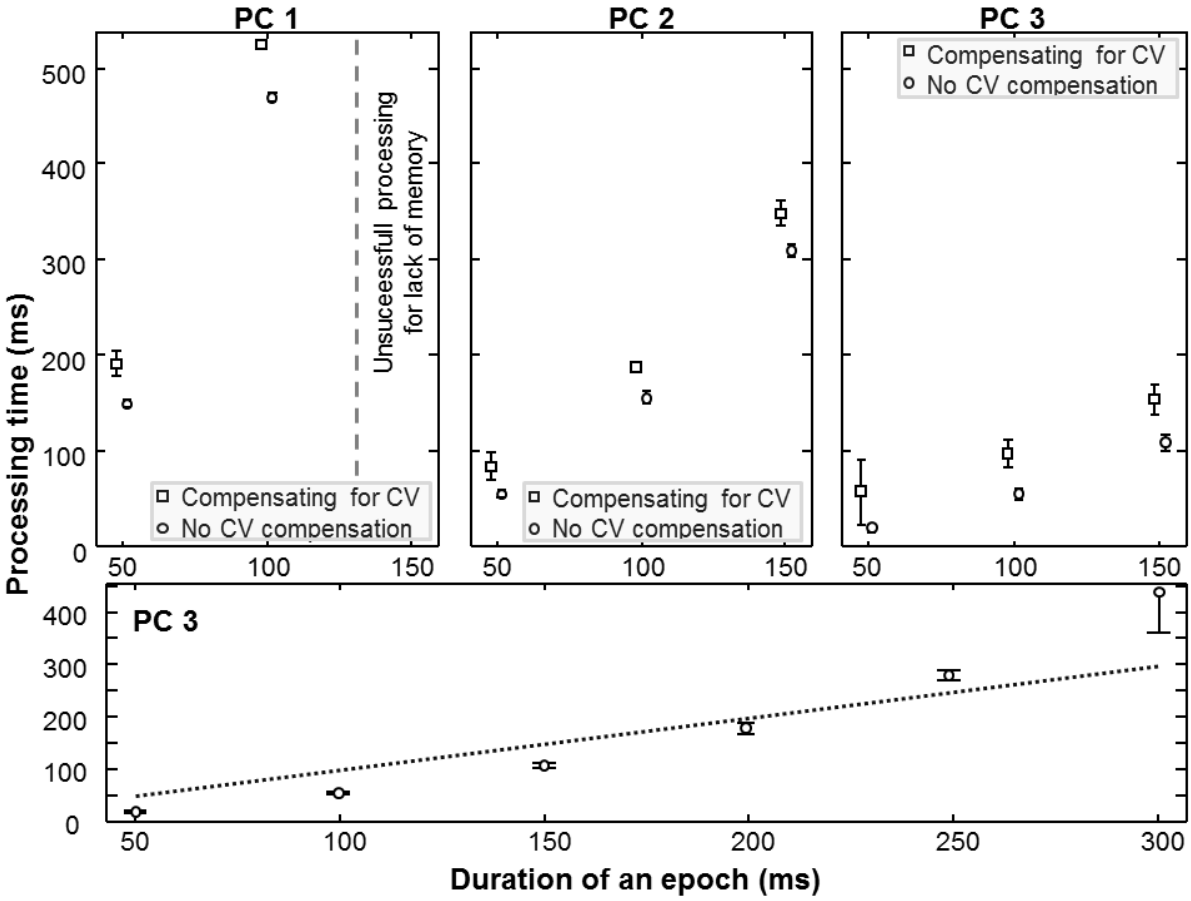

Figure 7. Processing time (mean and standard deviation) of epochs of different durations obtained using three personal computers (with performances indicated in Section 2.3). At the bottom, PC 3, the most performing personal computer, is tested further till the time required to process the data is larger than the duration of the epoch (the dot line indicates a processing time equal to the epoch duration).

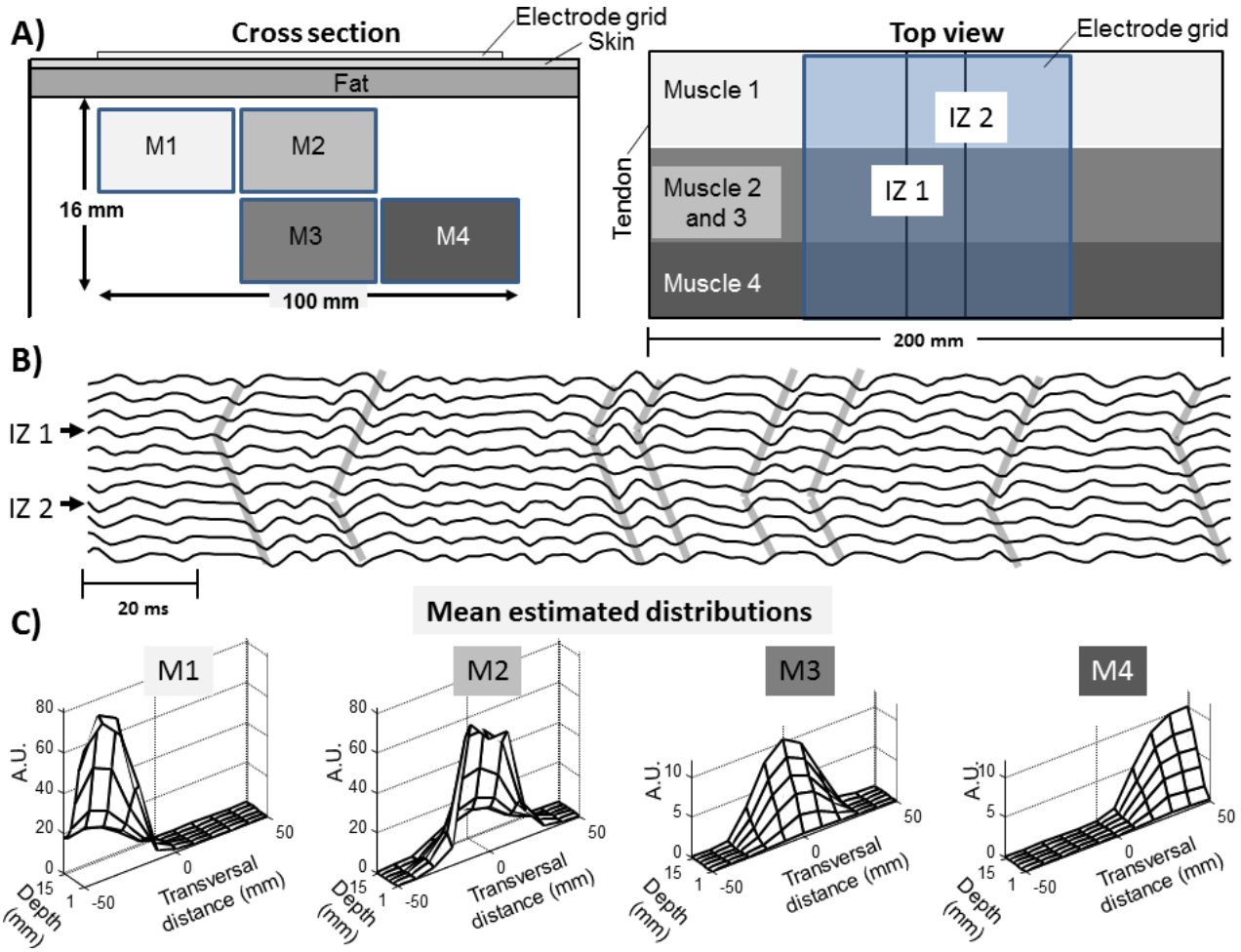

Figure 8. Test of the algorithm in the identification of the activity of different muscles. A) Geometry of the volume conductor and position of the detection grid. B) Portion of simulated signal (generated by muscle M2, recorded by the central column aligned to the fibres with IED of 5 mm). Some MUAPs are indicated, showing the different directions of propagation due to the presence of 2 distinct IZs. C) Mean distributions estimated from 5 s of signals simulating the selective contraction of each of the 4 muscles.